



Manipulation of microstructure in laser additive manufacturing

Shuang Bai¹ · Lihmei Yang¹ · Jian Liu¹

Received: 15 March 2016 / Accepted: 23 March 2016
© Springer-Verlag Berlin Heidelberg 2016

Abstract In this paper, additive manufacturing (AM) of tungsten parts is investigated by using femtosecond fiber lasers. For the first time, manipulating microstructures of AM parts is systematically investigated and reported. Various processing conditions are studied, which leads to desired characteristics in terms of morphology, porosity, hardness, and microstructural and mechanical properties of the processed components. Fully dense tungsten part with refined grain and increased hardness was obtained for femtosecond laser, compared with parts made with different pulse widths and CW laser. Micro-hardness is investigated for the fabricated samples. This can greatly benefit to the make of complicated structures and materials that could not be achieved before.

1 Introduction

Additive manufacturing (AM), especially laser aided AM, has attracted lots of attentions in the past two decades [1]. Laser AM of metal parts is among the most intensively studied in recent years [2, 3]. Currently, high-power continuous-wave (CW) lasers are widely used, along with some long-pulsed lasers (nanosecond to millisecond pulse duration) [3, 4]. Though many breakthroughs have been achieved, there are still many challenges to overcome, such as lack of accuracy due to the large heat affected zone, and limited type of materials [5]. Especially for high-temperature ($>3000\text{ }^{\circ}\text{C}$) material with high thermal conductivity

($>100\text{ W}(\text{mK})^{-1}$), like tungsten [6] and some ceramics [7], extremely high fluence will be needed to achieve fully melting of the samples.

Recently, we reported, for the first time, fs fiber laser is used to melt materials with extremely high melting temperature [8, 9]. In those study, single layer of powders was used to demonstrate the feasibility of full melting of high-temperature materials like tungsten (melting temperature $3422\text{ }^{\circ}\text{C}$), rhenium ($3182\text{ }^{\circ}\text{C}$) and some ultra-high-temperature ceramics ($>3000\text{ }^{\circ}\text{C}$). And various shaped parts (rings and cubes) of iron and tungsten were additively made with fs fiber laser. Those demonstrations showed a great promise of adopting fs fiber lasers in AM.

In this work, we further investigate the microstructure manipulation systematically in laser AM, for the first time. Tungsten powders were used with powder bed approach. Mechanical properties and microstructure of the fabricated parts were investigated in details by varying pulse width from 800 fs to 200 ps and compared with CW laser. The part fabricated by fs fiber laser showed greater hardness and smaller grain size than those made with picosecond or CW laser-processed samples.

2 Experimental setup

In our experiments, two types of lasers—femtosecond and CW—were integrated in one set and are switchable. They are 80 MHz pulse repetition rate fs Yb fiber laser (Uranus, Laser-Femto, Inc., California) and continuous-wave Yb fiber laser. The lasers have a central wavelength of 1030 nm. The 80 MHz laser has the full-width half-maximum (FWHM) pulse duration of 800 fs at an average power of 220 W, and the pulse width can be tuned from 800 fs to 200 ps. A homebuilt selective laser melting setup (powder

✉ Jian Liu
jianliu@polaronyx.com

¹ PolarOnyx, Inc., 2526 Qume Drive, Suite 17, San Jose, CA 95131, USA

bed) was used for the test (Fig. 1). The laser beam was guided through an acoustic-optical modulator (AOM), which was used to control the laser on/off and variation of the laser power. A laser scanner, equipped with an F-theta lens (100-mm-long focal length), was synchronized with the AOM and used to scan the laser beam on the powder surface. The scanner was mounted on a motorized stage to control the focal condition of the laser beam relative to the powder surface. The powders were evenly distributed on a substrate with a blade. The sample container was mounted on a z -stage and filled with argon gas to prevent oxidation. After one layer of powder was scanned, the sample container was lowered by a certain distance and a new layer of powders was deposited onto it using the blade. The newly deposited powder surface remained the same level as the previous one.

A variety of tungsten powders (10–50 μm , Atlantic Equipment Engineering, New Jersey) were used in our experiment. Five-mm-thick tungsten plates were used as the substrates. Parts with the cubic shape were fabricated.

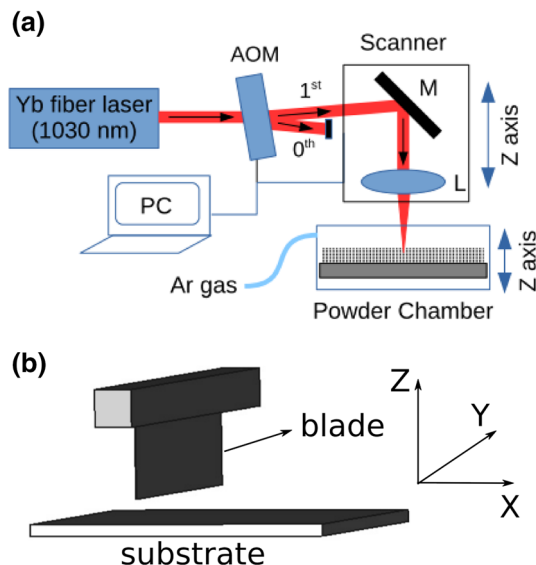
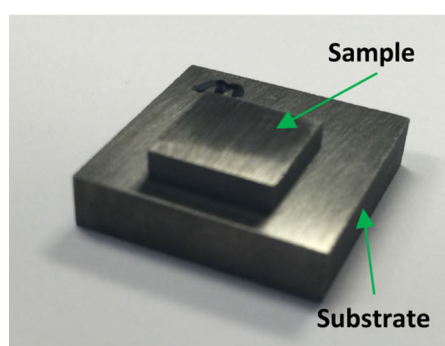


Fig. 1 Sketch of experimental setup. **a** Parts and layout of experimental setup. *AOM* acoustic-optical modulator, *M* galvanic mirrors. **b** Sketch of powder bed distribution

Fig. 2 Fully dense tungsten cube on tungsten substrate and convention used in interpretation of test results



The experiment parameters, such as scanning speed and focal condition, were varied and optimized to achieve the highest density. The processed samples were characterized and analyzed with EDS (IXRF 500), optical microscope imaging, micro-hardness (Buehler Micromet 2004), and grain structures [8, 9].

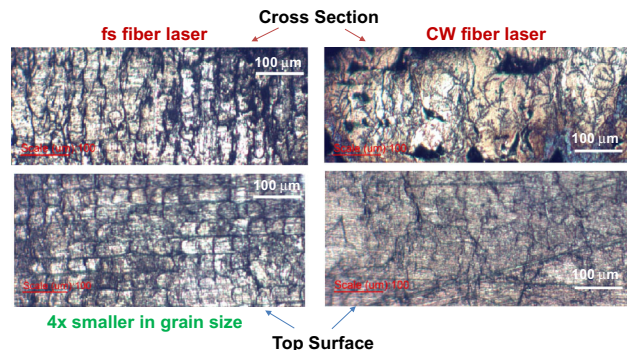


Fig. 3 fs fiber laser AM of tungsten powders has smaller grain size and controllable microstructures

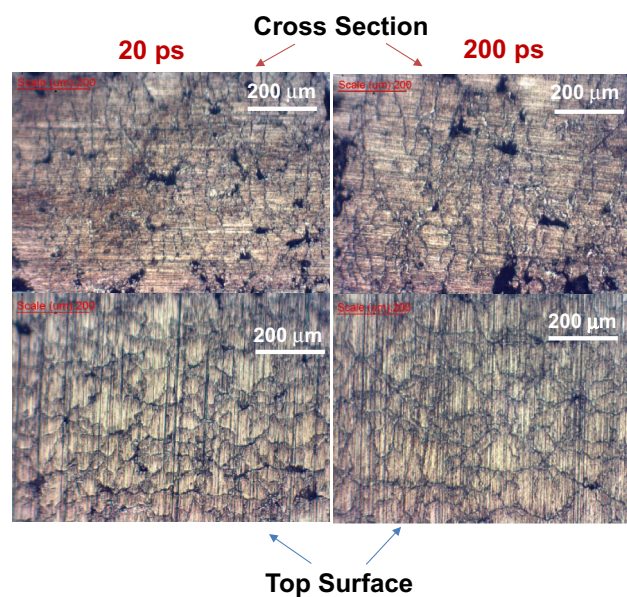
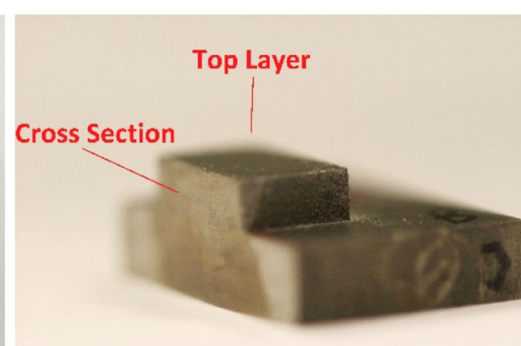


Fig. 4 Grain structure comparison for 20 ps (left) and 200 ps (right)



3 Results and discussion

A series of tungsten cubes (Fig. 2) were made by varying the pulse width to be 750 fs, 20, 200 ps, and CW mode, while keeping other AM parameters (such as laser power, scan speed, and focal condition) unchanged. After making

the tungsten cube samples, all of those samples including tungsten substrate were cut and polished first and then etched by solution (1 g NaOH and 1 g $K_3Fe(CN)_4$ into 10 mL water) for 3 min. After water rinse, alcohol rinse, and dry, microscopic image ($10\times$) for both sample and substrate surface was taken to measure the grain size. The

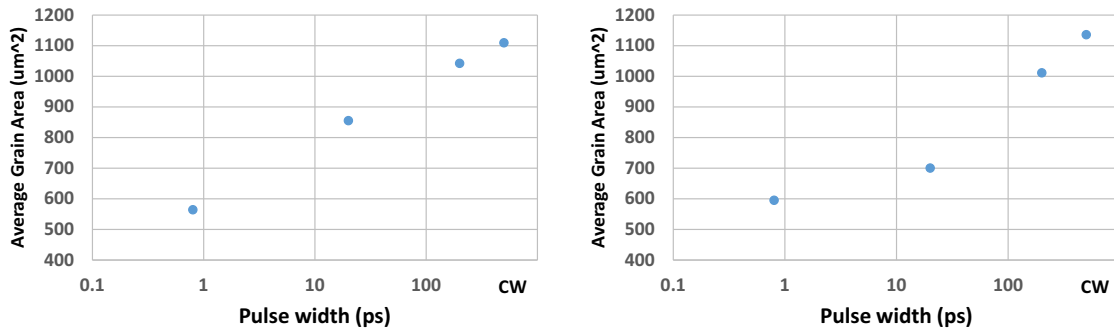


Fig. 5 Average grain size as function of pulse width. *Left* top surface. *Right* cross section

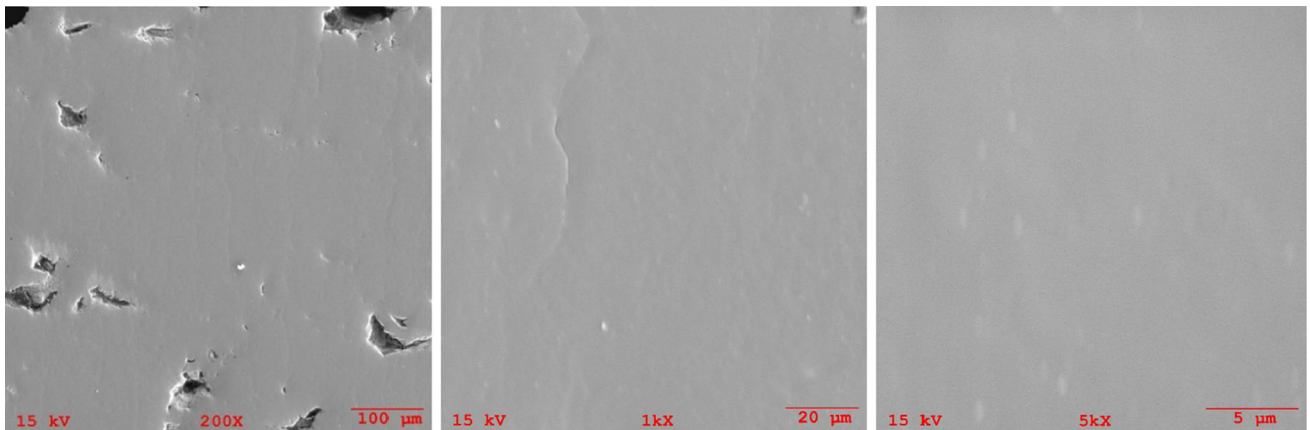


Fig. 6 Cross section of tungsten sample made by fs fiber laser, from *left* to *right*, SEM image of $\times 200$, $\times 1000$, $\times 5000$

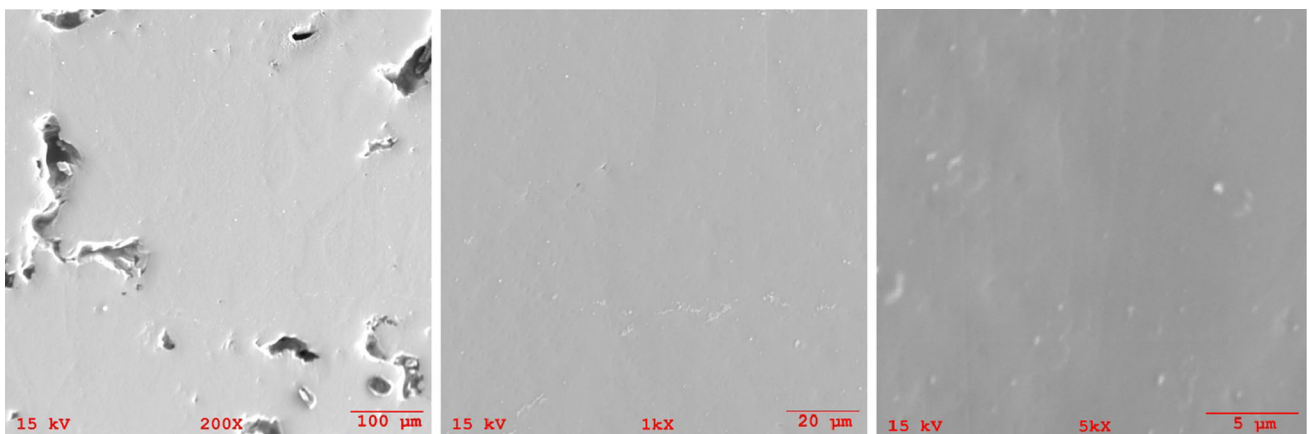


Fig. 7 Cross section of tungsten sample made by 20 ps laser, from *left* to *right*, SEM image of $\times 200$, $\times 1000$, $\times 5000$

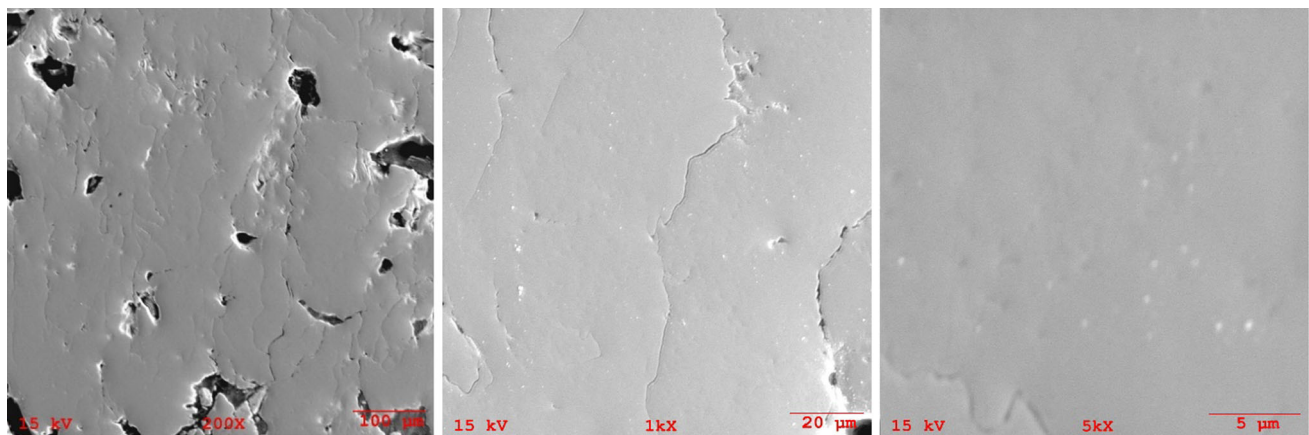


Fig. 8 Cross section of tungsten sample made by 200 ps laser, from *left* to *right*, SEM image of $\times 200$, $\times 1000$, $\times 5000$

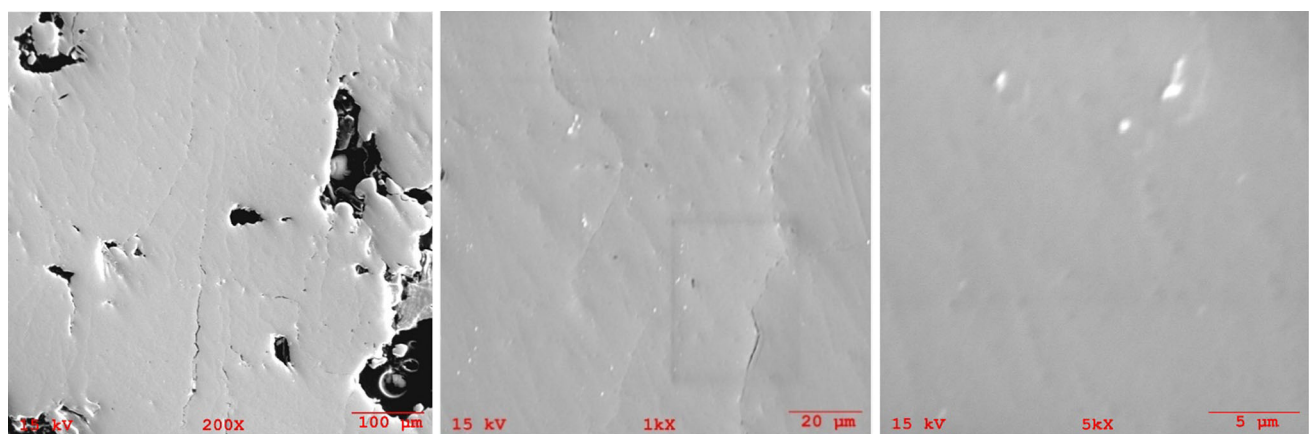


Fig. 9 Cross section of tungsten sample made by CW laser, from *left* to *right*, SEM image of $\times 200$, $\times 1000$, $\times 5000$

Table 1 Summary of the hardness testing results for different samples

Hardness (HRC)	fs sample	20 ps sample	200 ps sample	CW sample	Tungsten substrate
Top	45.4	44.1	42.4	44.7	44.9
Cross section	47.7	41.8	45.1	44.9	45.8

samples are further polished for taking SEM images. Figure 2 also illustrates the convention we used to describe the measurement results.

Comparison between fs laser and CW laser was made. Figure 3 shows the grain size comparison. Interestingly, the fs fiber laser-based AM can manipulate the microstructure and grain size and obtain as much as 4× smaller grain size than that of CW laser.

Further detailed comparison has been made by tuning the pulse width to 20 and 200 ps. Figure 4 shows example of the grain structure photographs. Using ImageJ, we calculated the average grain areas of fs, 20, 200 ps, CW laser AM samples and show the average results of five samples for each pulse width in Fig. 5. It clearly indicates that by tuning the pulse width, the grain size or microstructure can

be manipulated. And shorter pulse width produces smaller grain size, which is related to better mechanical strength (inversely proportional to the grain size) [10].

SEM images of tungsten samples made with 800 fs, 20, 200 ps, and CW laser were taken. As an example, cross-sectional SEM images are shown in Figs. 6, 7, 8, and 9. It does show that the fs laser-based AM generates less and smaller cracks and defects compared with those AM parts made with longer-pulsed or CW lasers. This is mainly because the melting characteristics (such as melting pool, heating rate, and possible cooling rate) induced by higher peak power of fs laser are much higher in rate and confined (melting pool) than long-pulsed lasers. Further investigation is ongoing to see whether there are any other factors involved.

Hardness testing was carried out with the micro-hardness testing instrument: Buehler Micromet 2400; Model: 1600-4987 (testing method: 200 g load and 10 s dwell time). Both the top layer and cross section of tungsten samples made with fs, 20, 200 ps, CW laser, and the tungsten substrate were measured and averaged over five different locations for each sample and five samples for each case. The data are summarized in Table 1. The hardness number of the fs sample is in general larger than those of long-pulsed and CW samples.

4 Conclusion

For the first time, we have demonstrated the microstructure or grain size of the AM parts can be manipulated or modified by varying laser parameters such as pulse width. This indicates that the mechanical properties are able to be tailored or modified either during the same part making process or at different parts making process, by varying laser parameters. It was shown that fs laser achieved the best results for tungsten samples on tungsten substrates in terms of microstructures and mechanical properties. This is mainly because the melting characteristics induced by higher peak power of fs laser are much higher in heating rate and cooling rate and are much more confined in melting pool than long-pulsed lasers and CW lasers. This finding is not only very important for the fabricating high-temperature materials such as tungsten but also important to other materials such as Al alloy, steels, Ti alloys, and ceramics. This will benefit automobile, aerospace, and

biomedical industries that demand products of superior mechanical properties and accuracy.

References

1. J. Kruth, Material incress manufacturing by rapid prototyping techniques. *CIRP Ann. Technol.* **40**, 603–614 (1991)
2. G.K. Lewis, E. Schlienger, Practical considerations and capabilities for laser assisted direct metal deposition. *Mater. Des.* **21**, 417–423 (2000)
3. J.P. Kruth, L. Froyen, J. Van Vaerenbergh, P. Mercelis, M. Rombouts, B. Lauwers, Selective laser melting of iron-based powder. *J. Mater. Process. Technol.* **149**, 616–622 (2004)
4. F. Abe, K. Osakada, M. Shiomi, K. Uematsu, M. Matsumoto, The manufacturing of hard tools from metallic powders by selective laser melting. *J. Mater. Process. Technol.* **111**, 210–213 (2001)
5. W.Y. Yeong, C.Y. Yap, M. Mapar, C.K. Chua, State-of-the-art review on selective laser melting of ceramics. in *High Value Manufacturing: Advanced Research in Virtual and Rapid Prototyping: Proceedings of the 6th International Conference on Advanced Research in Virtual and Rapid Prototyping, Leiria, Portugal, 1–5 October, 2013* (2013), p. 65
6. E. Lassner and W. Schubert, *Tungsten: Properties, Chemistry, Technology of the Elements, Alloys, and Chemical Compounds* (Kluwer Academic, New York, 1999)
7. J.M. Lonergan, W.G. Fahrenholtz, G.E. Hilmas, Zirconium diboride with high thermal conductivity. *J. Am. Ceram. Soc.* **97**, 1689–1691 (2014)
8. B. Nie, H. Huang, S. Bai, J. Liu, Femtosecond laser melting and resolidifying of high-temperature powder materials. *Appl. Phys. A* **118**(1), 37–41 (2015)
9. B. Nie, L. Yang, H. Huang, S. Bai, P. Wan, J. Liu, Femtosecond laser additive manufacturing of iron and tungsten parts. *Appl. Phys. A* **119**(3), 1075–1080 (2015)
10. A.C. Reardon, *Metallurgy for the Non-metallurgist*, Second Edition (ASM international, Materials Park, OH, 2011)